# Artificial Neural Network Based Design and Performance of Three-Phase Solar PV Integrated UPQC

Rahul. S. Jadhav[1], Chinnala. H. Mallareddy[2]
[1] *Student, FABTECH College of Engineering and Research, Sangola*
[2] *Professor, FABTECH College of Engineering and Research, Sangola*

***Abstract*- This paper deals with the Artificial Neural Network based design and the performance analysis of the three-phase solar photovoltaic integrated with unified power quality conditioner (PV-UPQC). It consist of the series voltage compensator and the shunt voltage compensator, both these compensators are connected back to back with a common DC-link. The shunt compensator extracts the power from PV array and also compensates the load current harmonics. To improve the performance of the PV-UPQC moving average filter is used to extract the load active current component based on the improved synchronous reference frame control. The grid side power quality problems of voltage swell and voltage sag are compensated with the help of series compensator. During the power quality problems such as voltage sag and swell condition the compensator injects voltage in-phase/out of phase respectively with point of common coupling (PCC). This proposed system leads to the combination of both the benefits of improvement in the power quality as well as clean energy generation. The dynamic performance as well as the steady state performance is evaluated by simulating in the MATLAB-Simulink.**

**Index terms- Artificial Neural Network, Series compensator, shunt compensator, Solar PV, UPQC, Power Quality, MPPT**

## I. INTRODUCTION

As the solar energy is surplus and easily available in the most part of the world, it has become the most important source of the renewable energy. It's the energy source which is free from the greenhouse effect. Hence the solar photovoltaic (PV) arrays are one the cleanest source of the renewable energy and the recent advances in solar manufacturing have increased the efficiency of the panels. Advancement in the semiconductor technology has increased the penetration of power electronics loads. The various loads such as computer power supplies, switched mode power supplies, adjustable speed drives etc. These loads have very good efficiency and however they draw nonlinear currents. These nonlinear currents lead to the voltage distortion at point of common coupling particularly in distribution systems.

The demand for the emphasis on clean energy generation is also increasing through the installation of PV system in commercial sectors as well as small apartments [1], [2]. The eco-friendly nature of the PV energy source has increased the penetration of such system, mainly in the weak distribution system leads to overcome the voltage quality problems like voltage sags and swell, which eventually causes instability in the grid [3]-[7]. These voltage quality problems also lead to frequent false tripping of power electronic systems, malfunctioning and false triggering of electronic systems and increased heating of capacitor banks etc [8]–[10].The major problems faced by distribution system at the grid side and load side are the power quality issues. Due to the demand for clean energy as well as stringent power quality requirement of sophisticated electronic loads, there is need for multifunctional systems which can integrate clean energy generation along with power quality improvement. A three phase multi-functional solar energy conversion system, which compensates for load side power quality issues, has been proposed in [11], [12].

Major research work has been done in integrating clean energy generation along with shunt active filtering. Though shunt active filtering has capability for both load voltage regulation, it comes at the cause of injecting reactive power. Thus shunt active filtering cannot regulate PCC voltage as well as maintain grid current unity power factor at same time. Recently, due to the stringent voltage quality

requirements for sophisticated electronics loads, the use of series active filters has been proposed for use in small apartments and commercial buildings [15], [16].

A solar photovoltaic system integrated along with dynamic voltage restorer has been proposed in [17]. Compared to shunt and series active power filters, a unified power quality conditioner (UPQC), which has both series and shunt compensators can perform both load voltage regulation and maintain grid current sinusoidal at unity power factor at same time. Integrating PV array along with UPQC, gives the dual benefits of clean energy generation along with universal active. The integration of PV array with UPQC has been reported in [18]–[20]. Compared to conventional grid connected inverters, the solar PV integrated UPQC has numerous benefits such as improving power quality of the grid, protecting critical loads from grid side disturbances apart from increasing the fault ride through capability of converter during transients.

With the increased emphasis on distributed generation and micro grids, there is a renewed interest in UPQC systems [21], [22].Reference signal generation is a major task in control of PVUPQC. Reference signal generation techniques can be broadly divided into time-domain and frequency domain techniques [8]. Time domain techniques are commonly used because of lower computational requirements in real-time implementation. The commonly used techniques include instantaneous reactive power theory (p-q theory), synchronous reference frame theory (d-q theory) and instantaneous symmetrical component theory [23].

The main problem in using the synchronous reference frame theory based method is that during the load unbalanced condition; double harmonic component is present in the d-axis current. Due to this, low pass filters with very low cut off frequency is used to filter out double harmonic component. This results in poor dynamic performance [24]. In this work, a moving average filter (MAF) is used to filter the d-axis current to obtain fundamental load active current. This gives optimal attenuation and without reducing the bandwidth of the controller [25]. Recently, MAF has been applied in improving performance of DC-link controllers as well as for grid synchronization using phase locked loop (PLL).

In this paper, the design and performance analysis of a three phase PV-UPQC are presented. An MAF based d-q theory based control is used to improve the dynamic performance during load active current extraction. The main advantages of the proposed system are as follows,

- Integration of clean energy generation and power quality improvement.
- Simultaneous voltage and current quality improvement.
- Improved load current compensation due to use of MAF in d-q control of PV-UPQC.
- Stable under various dynamic conditions of voltage sags/swells, load unbalance and irradiation variation.

The performance of the proposed system is analysed extensively under both dynamic and steady state conditions using MATLAB-Simulink software.

## II. DESIGN AND SYSTEM CONFIGURATION

The Fig.1 shows the structure for the PV-UPQC. The PV-UPQC shown in Fig.1 is designed for the three-phase system. It consists of series and the shunt compensators which are connected back to back with a common DC-link. The power quality issues at the load side are compensated as the shunt compensator is connected at the load side. The solar photovoltaic array is integrated directly to the DC-link of UPQC with the help of reverse blocking diode.

The power quality issues such as voltage sag/swell at the grid side are compensated with the help of series compensator which operates in the voltage control mode. Interfacing inductor is used to integrate the series and shunt compensators to the grid. A series injection transformer plays the important role in injecting the voltage generated by the series compensator into the grid with the help of interfacing inductors. Due to the switching operation of converters harmonics are generated which are filtered out with the help of Ripple filters. A nonlinear load is used consisting of bridge rectifier with a voltage-fed load. The load used is a nonlinear load consisting of a bridge rectifier with a voltage-fed load.

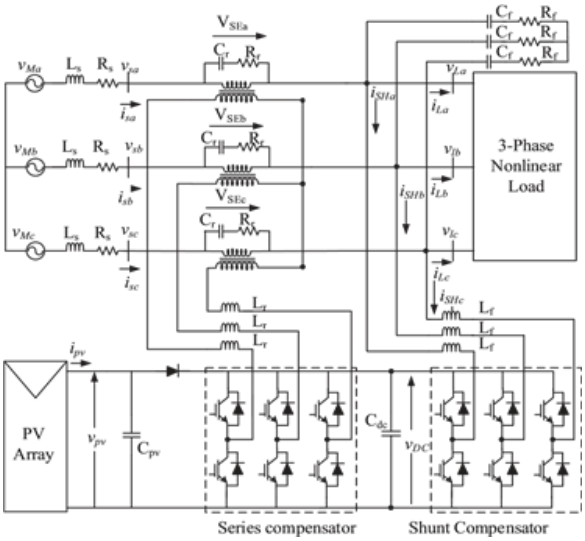


Figure1: Configuration system of PV-UPQC

A. Designing the PV-UPQC.

The designing of the PV-UPQC mainly includes the proper sizing of the PV array, DC-Link voltage level, Dc-Link capacitor, etc. The designing of the shunt compensator is sized in such a way it withstand the peak power output from the array and also compensates the load current reactive power and current harmonics. The PV array design size is such that the MPP voltage is same as that of the DC link voltage, because the PV array is integrated directly to DC-link of the UPQC. The PV array is rated in such a way that, under nominal condition feeds the power into the grid and also supplies the load active power. The other components which are designed are the series injection transformer of series compensator and the interfacing inductors of series and shunt compensator. The designing of the PV-UPQC is evaluated as follows.

1) Magnitude of DC-Link Voltage:-

It is denoted by Vdc and depends on the modulation depth used and the per-phase voltage of the system. The DC-link voltage magnitude should more than double the peak of per-phase voltage of the three phase system and is given as,

$$V_{dc} = \frac{2\sqrt{2}V_{LL}}{\sqrt{3}m}$$

Where, m is the modulation depth VLL is the grid line current. The modulation depth (m) is taken as unity(1). For the line voltage of 415 V, the minimum required value of the DC-bus voltage is 677.7 V. So, the voltage for the DC-bus is set at 700 V(approx.), which is same as that of the MPPT operating voltage of the PV array.

2) Capacitor Rating for the DC-Bus:

Depending upon the power requirement and the level of the DC-bus voltage the DC-link capacitor is sized. The DC-bus capacitor energy balance equation is given as follows,

$$C_{dc} = \frac{3kaV_{ph}I_{sh}t}{0.5 \times (V^2_{dc} - V^2_{dc1})}$$

$$= \frac{3 \times 0.1 \times 1.5 \times 239.6 \times 34.5 \times 0}{0.5 \times (700^2 - 677.79^2)}$$

$$= 9.3mF \quad (2)$$

where $V_{dc}$ is the average DC-bus voltage, $V_{dc1}$ is the lowest required value of DC-bus voltage, $a$ is the overloading factor, $V_{ph}$ is per-phase voltage, $t$ is the minimum time required for attaining steady value after a disturbance, $I_{sh}$ is per-phase current of shunt compensator, k is the factor that considers the variations in energy at the time of dynamics.

The minimum required DC-link voltage is $V_{dc1}$ = 677.69 V as obtained from (2), $V_{dc}$ = 700 V, $V_{ph}$= 239.60 V, $I_{sh}$=57.5 A, t= 30ms, a = 1.2, and for dynamic energy change = 10%, k= 0.1, the value of $C_{dc}$ is obtained as 9.3 mF.

3) Shunt Compensator Interfacing Inductor:-

The rating of the interfacing inductor of the shunt compensator depends upon the ripple current and the DC- link voltage switching frequency. The equation for the interfacing inductor is given as follows,

$$L_f = \frac{\sqrt{3}mV_{dc}}{12af_{sh}I_{cr,pp}}$$

$$= \frac{\sqrt{3} \times 1 \times 700}{12 \times 1.2 \times 10000 \times 6.9}$$

$$= 800\mu H \approx 1mH \quad (3)$$

where $m$ is depth of modulation, a is pu value of maximum overload, $f_{sh}$ is the switching frequency , $I_{cr,pp}$ is the inductor ripple current which is taken as 20% of rms phase current of shunt compensator. Here, m=1, a=1.2, $f_{sh}$=10kHz, $V_{dc}$=700V, one gets

800 $\mu$H as value. The value chosen is approximated to 1mH.

4) Series Injection Transformer:-

The PV-UPQC is designed to compensate for a sag/swell of 0.3 pu i.e 72V. Hence, the required voltage to be injection is only 72V which results in low modulation index for the series compensator when the DC-link voltage is 620V. In order to operate the series compensator with minimum harmonics, one keeps modulation index of the series compensator near to unity. Hence a series transformer is used with a turn's ratio,

$$K_{SE} = \frac{V_{VSC}}{V_{SE}} = 3.33 \approx 3 \quad (4)$$

The value obtained for KSE is 3.33. The value selected is 3. The rating of series injection transformer is given as,

$$S_{SE} = 3V_{SE}I_{SEsag} = 3\times72\times46 = 10kVA \quad (5)$$

The current through series VSC is same as grid current. The supply current under sag condition of 0.3 pu is 46 A and hence the VA rating of injection transformer achieved is 10 kVA.

5) Interfacing Inductor of Series Compensator:

The rating of interfacing inductor of the series compensator depends on ripple current at swell condition, switching frequency and DC-link voltage. Its value is expressed as,

$$L_x = \frac{\sqrt{3}\times mV_{dc}K_{SE}}{12af_{se}I_r}$$

$$= \frac{\sqrt{3}\times 1\times 700\times 3}{12\times 1.2\times 10000\times 7.1}$$

$$= 3.6mH \quad (6)$$

where m is the depth of modulation, a is the pu value of maximum overload, $f_{se}$ is the switching frequency, $I_r$ is the inductor current ripple, which is taken to be 20% of grid current. Here, m=1, a=1.5, $f_{se}$=10 kHz, $V_{dc}$=700 V and 20% ripple current, one gets 3.6 mH as selected value.

## III. CONTROL OF PV-UPQC

The two main subsystems for the PV-UPQC are the series and shunt compensator. The load side power quality problems such as load current harmonics and the load reactive power are compensated by the shunt compensator. In case of PV-UPQC, the shunt compensator performs the additional function of supplying power from the solar PV array. The shunt compensator extracts power from the PV-array by using a maximum power point tracking (MPPT) algorithm. The series compensator protects the load from the grid side power quality problems such as voltage sags/swells by injecting appropriate voltage in phase with the grid voltage.

### *A. Control of Shunt Compensator*

The shunt compensator extracts the maximum power from the solar PV-array by operating it at its maximum power point. The maximum power point tracking (MPPT) algorithm generates the reference voltage for the DC-link of PV-UPQC. Some of the commonly used MPPT algorithms are Perturb and Observe (P& O) algorithm, incremental conductance algorithm (INC). In this work, (P& O) algorithm is used for implementing MPPT. The DC-link voltage is maintained at the generated reference by using a PI-controller.

To perform the load current compensation, the shunt compensator extracts the active fundamental component of the load current. For this work, the shunt compensator is controlled by extracting fundamental active component of load current using SRF technique. The control structure of shunt compensator is shown in Fig. 2. The load currents are converted to d-q-0 domain using the phase and frequency information obtained from PLL. The PLL input is the PCC voltage. The d-component of the load current ($I_{Ld}$) is filtered to extract DC component ($I_{Ldf}$) which represents the fundamental component in abc frame of reference. To extract DC component without deteriorating the dynamic performance, a moving average filter (MAF) is used to extract the DC component. The transfer function of moving average filter is given

$$MAF(s) = \frac{1- e^{-Tws}}{T_{ws}} \quad (7)$$

where $T_w$ is the window length of the moving average filter. As the lowest harmonic present in the d-axis current is double harmonic component, $T_w$ is kept at

half of fundamental time period. The MAF has unity DC gain and zero gain integer multiples of window length.The equivalent current component due to PV array is given as,

$$I_{pvg} = \frac{2}{3}\frac{P_{pv}}{V_s} \quad (8)$$

where $P_{pv}$ is the PV array power and $V_s$ is the magnitude of the PCC voltage. The reference grid current in d-axis is given as

$$I^*_{sd} = I_{Ldf} + I_{loss} - I_{pvg} \quad (9)$$

$I^*_{sd}$ is converted to abc domain reference grid currents. The reference grid currents are compared with the sensed grid currents in a hysteresis current controller to generate the gating pulses for the shunt converter.

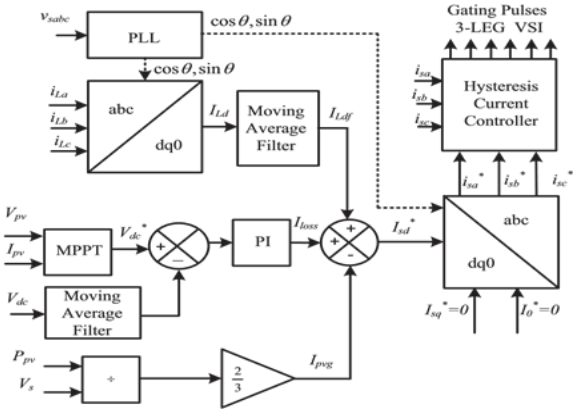


Figure 2: Control Structure of Shunt Compensator

B. Control of Series Compensator

The control strategies used for the series compensator are pre sag compensation, in-phase compensation and energy optimal compensation. Here the series compensator injects voltage in same phase as that of grid voltage, which results in minimum injection of voltage by the series compensator. The fig.3 shows the control structure for the series compensator. The fundamental component of PCC voltage is extracted using a PLL which is used for generating the reference axis in dq-0 domain. The reference load voltage is generated using the phase and frequency information of PCC voltage obtained using PLL. The PCC voltages and load voltages are converted into d-q-0 domain. As the reference load voltage is to be in phase with the PCC voltage, the peak load reference voltage is the d-axis component value of load reference voltage. The q-axis component is kept at zero. The difference between the load reference voltage and PCC voltage gives the reference voltage for the series compensator. The difference between load voltage and PCC voltage gives the actual series compensator voltages. The difference between reference and actual series compensator voltages is passed to the PI controllers for the generation of appropriate reference signals. These signals are converted to abc domain and then passed through pulse width modulation (PWM) voltage controller to generate appropriate gating signals for the series compensator.

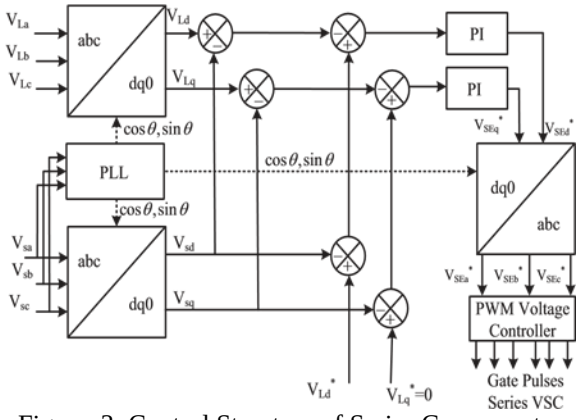


Figure 3: Control Structure of Series Compensator

C. Design of ANN Controller

The ANN-based controller is designed for the current control of the shunt active power filter and also trained offline using the data from the conventional proportional-integral controller. An exhaustive simulation study is carried out to investigate the performance of the ANN controller and compare its performance with the conventional PI controller results. The primary requirement for the desired compensation of UPQC are the rapid detection in the disturbance of the signal along with high accuracy, high dynamic response of the controller and quick processing of the reference signal. The conventional controller fails to perform satisfactorily under parameter variations nonlinearity load disturbance, etc. A recent study indicates that NN- based controller's gives quick dynamic response and also maintains the stability over a wide operating range of the converter system. ANN is made up of interconnecting various artificial neurons. ANN is essentially a cluster of suitably interconnected nonlinear elements of very simple form that possess

the ability to learn and adapt. It resembles the brain in two aspects:

1. Through the learning process the knowledge is acquired by the network.
2. To store knowledge the Interneuron connection strengths are used.

These networks are differentiated by their topology, the way in which they communicate with their environment, the manner in which they are trained, and their ability to process information. ANNs are used to solve the AI problems without necessarily creating a model of a real dynamic system.


Figure 4: Exploded diagram of the artificial neural network.

A multi-layer feed forward type ANN based controller is designed for the improvement in the performance of the UPQC. The network is so designed that it has three layers, such that the input layer with has 2 neuron, the hidden layer has 21 neuron, and the output layer has 1 neuron, respectively. The large data of the dc-link current for and intervals from the conventional method are collected and are stored in the MATLAB workspace. These data are used for training the NN. The activation functions chosen are tan sigmoidal for input and hidden layers and pure linear in the output layer, respectively. The multilayer feed forward type NN works as the compensation signal generator.

The training algorithm used is Levenberg–Marquardt back propagation (LMBP). The MATLAB programming for the NN training is given as follows:

```
net=newff (minmax (P) , [2,21,1] , {'tansig ' ,'tansig ' ,'purelin'},'trainlm');
net . trainParam . show=50;
net . trainParam . lr=0.05;
net . trainParam . mc=0.95;
net . trainParam . lr_inc=1.9;
net . trainParam . epochs=1000;
net . trainParam . goal=1e-6;
[net , tr]=train (net ,P,T);
a=sim (net , P);
gensim (net,-1);
```

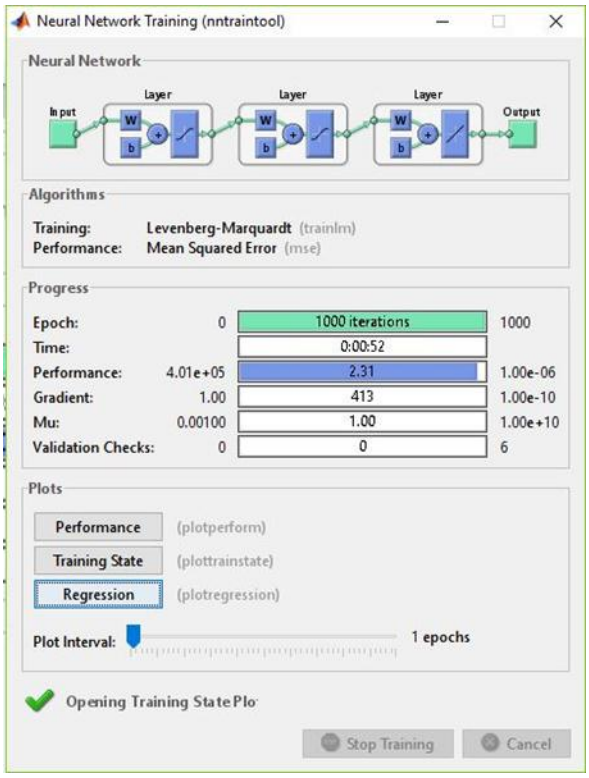


Figure 5: Neural Network Training (nn train tool)

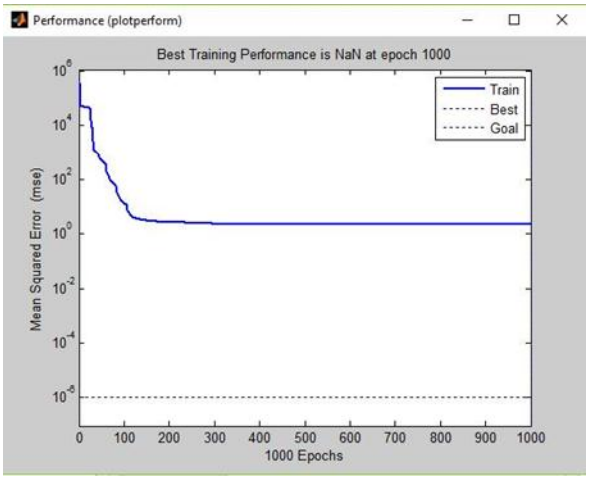


Figure 6: Performance

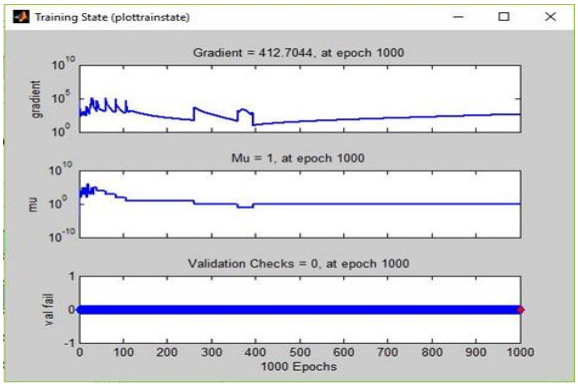


Figure 7: Training State

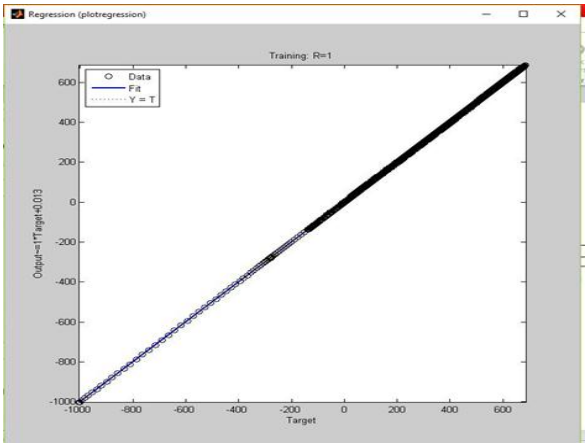


Figure 8: Regression

## IV. SIMULATION STUDIES

The steady state and dynamic performances of PV-UPQC are analysed by simulating the system in MATLAB-Simulink software. The load used is a nonlinear load which consist of three phase diode bridge rectifier with R-L load. The system is subjected to various dynamic conditions such as sag and swells in PCC voltage and PV irradiation variation.

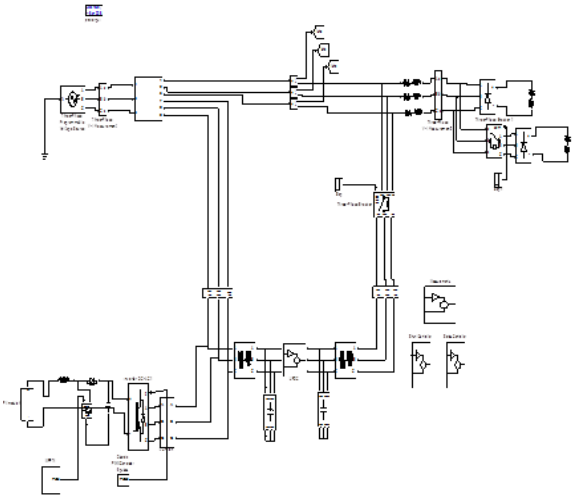

Figure 9: Simulation of Three-Phase Solar PV Integrated UPQC

## V. SIMULATION RESULTS

### A. Performance of PV-UPQC at PCC Voltage Fluctuations

The dynamic performance of the solar PV-UPQC under the conditions of PCC voltage sags/swells is shown in Fig.10. The irradiation (G) is kept at $600 W/m^2$. The various sensed signals are PCC voltages ($v_s$), load voltages($v_L$), series compensator voltages ($v_{SE}$), DC-link voltage ($V_{dc}$), grid currents ($i_S$), load currents ($i_{La}$). Between 0.1s and 0.2s, there is voltage sag/swell of 0.3pu i.e 72V. Hence, the required voltage to be injected is 72V which results in lower modulation index for the series compensator when the DC-Link voltage is 620V. The series compensator compensates the grid voltage under these conditions by injecting a suitable voltage $v_{SE}$ in opposite phase with the grid voltage disturbance to maintain the load voltage at rated voltage condition.

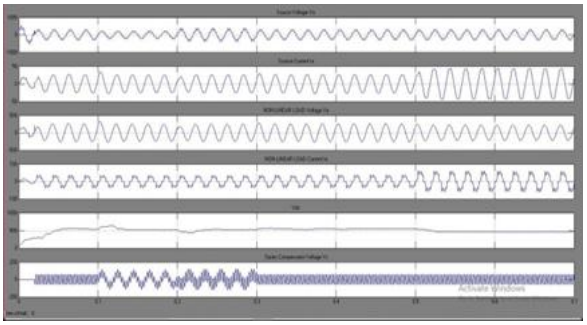

Figure 10: Performance of PV-UPQC under Voltage Sag and Swell Conditions.

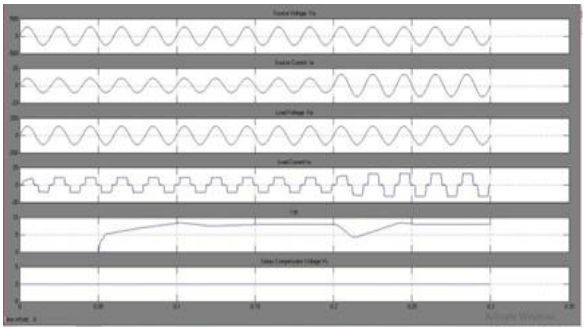

Figure 11: Artificial Neural Network based Performance of PV-UPQC under Voltage Sag and Swell Conditions.

### B. Harmonics Spectrum and Total Harmonic Distortion

The harmonic spectrum, THD of load current and the grid current without the Artificial Neural Network are shown in Fig. 12 and Fig.13. Similarly the Artificial Neural Network based harmonic spectrum, THD of load current and grid current are shown in Fig.14 and Fig.15. It has been that observed that the load current THD is 27.69% and grid current THD is 5.28% without ANN and the load current THD is 29.37% and grid current THD is 0.76% with Artificial Neural Network, thus meeting the requirement.

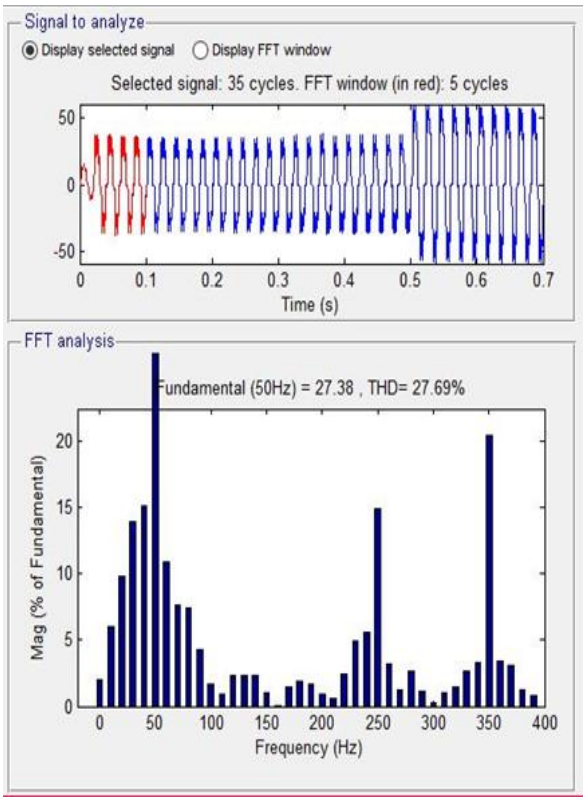


Figure 12: Harmonic Spectrum and THD of Load Current without Artificial Neural Network.

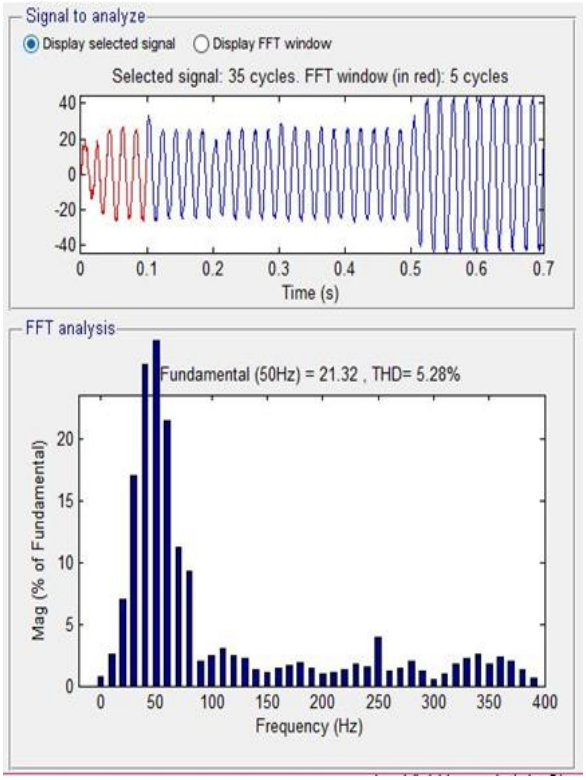


Figure 13: Harmonic Spectrum and THD of Grid Current without Artificial Neural Network

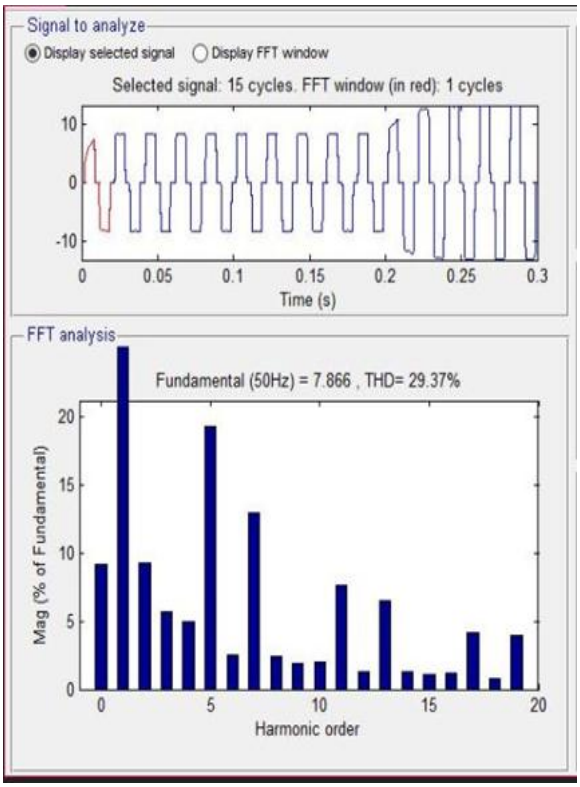


Figure 14: Artificial Neural Network BasedHarmonic Spectrum and THD of Load Current.

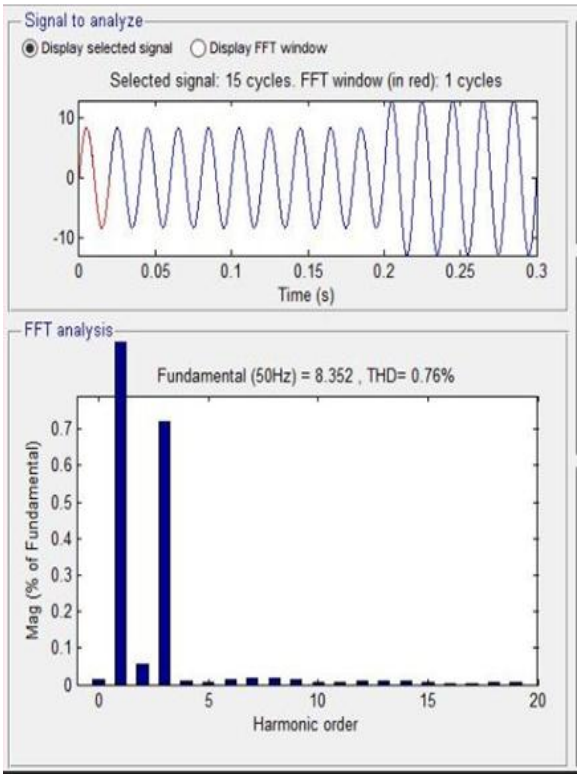


Figure 14: Artificial Neural Network Based Harmonic Spectrum and THD of Grid Current.

## VI. CONCLUSION

The design and the dynamic performance of three-phase PV-UPQC have been analysed under the conditions of variable irradiation and grid voltage sags/swells. It has been that observed that PV-UPQC mitigates the harmonics caused by the nonlinear load and maintains the THD of grid current under limits. This system is found to be stable under the conditions of variation of irradiation, voltage sags/swell and load unbalance. The performance of d-q control particularly in the load unbalanced condition has been improved through the use of moving average filter. It can be seen that Artificial Neural Network based PV-UPQC is the good solution for the modern distribution system by integrating distributed generation with the improvement in power quality.

## REFERENCES


[1] B. Mountain and P. Szuster, "Solar, solar everywhere: Opportunities and challenges for australia's rooftop pv systems," IEEE Power and Energy Magazine, vol. 13, no. 4, pp. 53–60, July 2015.

[2] A. R. Malekpour, A. Pahwa, A. Malekpour, and B. Natarajan, "Hierarchical architecture for integration of rooftop pv in smart distribution systems," IEEE Transactions on Smart Grid, vol. PP, no. 99, pp. 1–1, 2017.

[3] Y. Yang, P. Enjeti, F. Blaabjerg, and H. Wang, "Wide-scale adoption of photovoltaic energy: Grid code modifications are explored in the distribution grid," IEEE Ind. Appl. Mag., vol. 21, no. 5, pp. 21–31, Sept 2015.

[4] M. J. E. Alam, K. M. Muttaqi, and D. Sutanto, "An approach for online assessment of rooftop solar pv impacts on low-voltage distribution networks," IEEE Transactions on Sustainable Energy, vol. 5, no. 2, pp. 663–672, April 2014.

[5] J. Jayachandran and R. M. Sachithanandam, "Neural network-based control algorithm for DSTATCOM under nonideal source voltage and varying load conditions," Canadian Journal of Electrical and Computer Engineering, vol. 38, no. 4, pp. 307–317, Fall 2015.

[6] A. Parchure, S. J. Tyler, M. A. Peskin, K. Rahimi, R. P. Broadwater, and M. Dilek, "Investigating pv generation induced voltage volatility for customers sharing a distribution service transformer," IEEE Trans. Ind. Appl., vol. 53, no. 1, pp. 71–79, Jan 2017.

[7] E. Yao, P. Samadi, V. W. S. Wong, and R. Schober, "Residential demand side management under high penetration of rooftop photovoltaic units," IEEE Transactions on Smart Grid, vol. 7, no. 3, pp. 1597–1608, May 2016.

[8] B. Singh, A. Chandra and K. A. Haddad, Power Quality: Problems and Mitigation Techniques. London: Wiley, 2015.

[9] M. Bollen and I. Guo, Signal Processing of Power Quality Disturbances. Hoboken: Johm Wiley, 2006.

[10] P. Jayaprakash, B. Singh, D. Kothari, A. Chandra, and K. Al-Haddad, "Control of reduced-rating dynamic voltage restorer with a battery energy storage system," IEEE Trans. Ind. Appl., vol. 50, no. 2, pp. 1295– 1303, March 2014.

[11] B. Singh, C. Jain, and S. Goel, "ILST control algorithm of singlestage dual purpose grid connected solar pv system," IEEE Trans. Power Electron., vol. 29, no. 10, pp. 5347–5357, Oct 2014.

[12] R. K. Agarwal, I. Hussain, and B. Singh, "Three-phase single-stage grid tied solar pv ecs using PLL-less fast CTF control technique," IET Power Electronics, vol. 10, no. 2, pp. 178–188, 2017.

[13] Y. Singh, I. Hussain, B. Singh, and S. Mishra, "Single-phase solar gridinterfaced system with active filtering using adaptive linear combiner filter-based control scheme," IET Generation, Transmission Distribution, vol. 11, no. 8, pp. 1976–1984, 2017.

[14] T.-F. Wu, H.-S. Nien, C.-L. Shen, and T.-M. Chen, "A single-phase inverter system for pv power injection and active power filtering with nonlinear inductor consideration," IEEE Trans. Ind. Appl., vol. 41, no. 4, pp. 1075–1083, July 2005.

[15] A. Javadi, A. Hamadi, L. Woodward, and K. Al-Haddad, "Experimental investigation on a hybrid series active power compensator to improve power quality of typical households," IEEE Trans. Ind. Electron., vol. 63, no. 8, pp. 4849–4859, Aug 2016.

[16] A. Javadi, L. Woodward, and K. Al-Haddad, "Real-time implementation of a three-phase thseaf based on vsc and p+r controller to improve power quality of weak distribution systems," IEEE Transactions on Power Electronics, vol. PP, no. 99, pp. 1–1, 2017.

[17] A. M. Rauf and V. Khadkikar, "Integrated photovoltaic and dynamic voltage restorer system configuration," IEEE Transactions on Sustainable Energy, vol. 6, no. 2, pp. 400–410, April 2015.

[18] S. Devassy and B. Singh, "Design and performance analysis of threephase solar pv integrated upqc," in 2016 IEEE 6th International Conference on Power Systems (ICPS), March 2016, pp. 1–6.

[19] K. Palanisamy, D. Kothari, M. K. Mishra, S. Meikandashivam, and I. J. Raglend, "Effective utilization of unified power quality conditioner for interconnecting PV modules with grid using power angle control method," International Journal of Electrical Power and Energy Systems, vol. 48, pp. 131 – 138, 2013.

[20] S. Devassy and B. Singh, "Modified p-q theory based control of solar pv integrated upqc-s," IEEE Trans. Ind. Appl., vol. PP, no. 99, pp. 1–1, 2017.

[21] S. K. Khadem, M. Basu, and M. F. Conlon, "Intelligent islanding and seamless reconnection technique for microgrid with upqc," IEEE Journal of Emerging and Selected Topics in Power Electronics, vol. 3, no. 2, pp. 483–492, June 2015.

[22] J. M. Guerrero, P. C. Loh, T. L. Lee, and M. Chandorkar, "Advanced control architectures for intelligent microgrids;part ii: Power quality, energy storage, and ac/dc microgrids," IEEE Transactions on Industrial Electronics, vol. 60, no. 4, pp. 1263–1270, April 2013.

[23] B. Singh and J. Solanki, "A comparison of control algorithms for dstatcom," IEEE Transactions on Industrial Electronics, vol. 56, no. 7, pp. 2738–2745, July 2009.

[24] B. Singh, C. Jain, S. Goel, A. Chandra, and K. Al-Haddad, "A multifunctional grid-tied solar energy conversion system with anf-based control approach," IEEE Transactions on Industry Applications, vol. 52, no. 5, pp. 3663–3672, Sept 2016.

[25] S. Golestan, M. Ramezani, J. M. Guerrero, and M. Monfared, "dq-frame cascaded delayed signal cancellation- based pll: Analysis, design, and comparison with moving average filter-based pll," IEEE Transactions on Power Electronics, vol. 30, no. 3, pp. 1618–1632, March 2015.